

Network pharmacology for deciphering molecular mechanism of mahogany in dyslipidemia treatment of menopausal conditions

Afivah Dewi Anggraeni, S. Farm¹, Dhiya Ulhaq Salsabila¹, Bayu Anggoro¹, Adam Hermawan, Dr. rer. nat.^{1,2}

¹Cancer Chemoprevention Research Center, Faculty of Pharmacy, Universitas Gadjah Mada, Yogyakarta Indonesia, ²Macromolecular Engineering Laboratory, Department of Pharmaceutical Chemistry, Faculty of Pharmacy, UGM, Yogyakarta, Indonesia

ABSTRACT

Introduction: Estrogen deficiency during menopause is associated with pathological menopausal syndromes and metabolic disorders, including dysregulated lipid metabolism (dyslipidemia). Mahogany is a promising material for use in an alternative treatment for preventing dyslipidemia during menopause. This study investigated the potency of mahogany compounds and their molecular mechanism as an alternative treatment for preventing dyslipidemia during menopause.

Method and Materials: The determination of the potential of the compounds of interest was performed by machine learning using KNIME software to identify the potential compounds for HMG-CoA Reductase (HMGCR) inhibitor. Target genes for a potential mahogany compound were obtained from Swiss Target Prediction. Analysis of the KEGG-Pathways, Gene Ontology profiling, and protein-protein interaction networks of the target gene were analyzed.

Results: We identified five compounds: β -sitosterol, swietemacrophyllanin, 7-hydroxy-2-(4-hydroxy-3-methoxyphenyl)-chroman-4-on (7-HMC), scopoletin, and stigmasterol as candidates for HMGCR inhibitors. The target prediction results mined 294 genes. The top 20 hub genes with the highest degree included MAPK1/3, PI3K/AKT, ER1, and mTOR, which played a role in lipid metabolism.

Conclusion: The possible molecular mechanisms mainly involved direct inhibitory pathway of HMGCR and an indirect inhibitory pathway of HMGCR. The tidal inhibitory pathway was indirectly mediated via the PI3K/AKT, MAPK1/3, MTOR, ER1, and SREBP1/2 signaling pathways. Further investigation is warranted to validate the results of the present study.

KEYWORDS:

Mahogany, Dyslipidemia, Menopause, HMG-CoA Reductase, and Bioinformatics

INTRODUCTION

Menopause is a condition of the cessation of the menstrual cycle in women as a result of aging of the reproductive

organs.¹ A new hormonal pattern is established at menopause, which is characterized by low estrogen level.² Estrogen is a steroid hormone produced primarily in the ovaries that contributes to the regulation of some physiological mechanisms. Estrogen deficiency during menopause is associated with pathological menopausal syndromes, psychiatric disorders, cardiovascular diseases (CVDs), cancer, and metabolic disorders, including dysregulated lipid metabolism or dyslipidemia.³ Hormone replacement therapy (HRT) using estrogen synthesis has been the primary treatment for preventing menopausal symptoms, CVD, and dyslipidemia.⁴ However, clinical studies have demonstrated that HRT increases the risks of endometrial and breast cancers and hence cannot be used as an idealized therapy.⁵ Seeking alternative dietary estrogenic compounds is believed to be crucial for the prevention of menopause-associated metabolic syndromes.⁶

Decreasing level of estrogen during menopause causes dyslipidemia through multiple mechanisms.⁷ Decreased level of estrogen increases the hepatic HMG-CoA reductase (HMGCR) gene expression and activation, leading to the elevation of the serum cholesterol levels.⁸ HMGCR is a rate-limiting enzyme that plays a pivotal role in cholesterol biosynthesis. Dysregulation of lipid metabolism during menopause can alter the level of various lipids circulating in the blood, such as lipoproteins, apolipoproteins, low-density lipoproteins (LDLs) high-density lipoproteins (HDL), and triacylglycerol (TG).⁹

Mahogany (*Swietenia macrophylla* and *Swietenia mahogany*) has the potential resource of phytoestrogen¹⁰ Mahogany has been used in the preparation of traditional medicine in Asia to treat hypertension, diabetes, and pain.¹¹ Chemical compounds in mahogany include flavonoids, saponins, alkaloids, steroids, and tannins. Recent studies have demonstrated that mahogany seeds have an estrogenic activity that can increase the uterine weight and bone density, prolong the estrus phase, and increase the breast gland proliferation in ovariectomized rats.¹² Another study also showed that compound contained in the mahogany extract could decrease the cholesterol, triglyceride, low-density lipoprotein, increased high-density lipoprotein, and reduced atherogenic indexes.¹³⁻¹⁵ According to the study performed by Kalpana and Pugalendi, the *in vivo* study of

Corresponding Author: Adam Hermawan
Email: adam_apt@ugm.ac.id

ethanolic extract of mahogany seeds on rats proved reduction in the level of total cholesterol, triglyceride, LDL, and VLDL and increase in the level of HDL.¹⁵ This finding suggests that mahogany offers potential efficacy for preventing menopause syndrome and hyperlipidemia that often occur during menopause.

Mahogany is a promising plant for use in preventing dyslipidemia during menopause. However, the detailed therapeutic targets and signaling mechanisms behind the benefits of mahogany remain unknown.¹³ Cholesterol in our body can arise from *de novo* synthesis in our cells or obtained through food consumption.¹⁶ In the process of cholesterol biosynthesis, 3-hydroxy-3-methylglutaryl coenzyme A (HMG-CoA) reductase (HMGCR) catalyzes HMG-CoA conversion to mevalonate. It is known as a rate-limiting enzyme in cholesterol synthesis, signifying its important role. The multivalent system regulates HMGCR through various mechanisms.¹⁷

This study was conducted to investigate the potency of mahogany compound's molecular targets and signaling mechanisms as an alternative treatment for preventing dyslipidemia during menopause by focusing on the indirect effects. In this study, bioinformatics analysis was performed to investigate the potential compound of mahogany that can inhibit HMGCR, an enzyme that plays an essential role in lipid metabolism. The use of bioinformatics analysis can simplify and organize bioinformatics data such that it allows researchers to access existing information and submit new entries as they are produced and make new conclusions and understand new possibilities. In conclusion, we identified and developed potential compound candidates and predicted their molecular target and molecular signaling role in lipid metabolism.

MATERIAL AND METHODS

Prediction inhibition activity prediction using KNIME

The prediction model for the inhibition of mahogany compounds against HMGCR was developed using the dataset inhibitor compound activity against HMGCR obtained from ChEMBL (<https://www.ebi.ac.uk/chembl>), which were entered in ChEMBL ID and analyzed by the KNIME version 4.3.1 with the pipeline/workflow created. Mahogany metabolite profiles were analyzed to predict the inhibitory activity on HMGCR based on the prediction model prepared. The outputs produced were the "ROC curve" and "Prediction value," which provided method validation and prediction value of mahogany's metabolites. Furthermore, the potential compounds in mahogany's metabolites were selected by identifying the compounds that predicted the inhibitory activity based on the machine learning (ML) prediction outcomes.¹⁸

Target prediction and collection

The potential compounds of mahogany metabolites were analyzed for their predictive target genes using online databases based on the SMILES code. The database used included Swiss Target Prediction (<http://www.swisstargetprediction.ch>) with the default settings. The total target genes were collected, combined, and then sliced using the InteractiVenn

(<http://www.interactivenn.net>) to ensure no duplicity in the target.¹⁹

Gene ontology (GO) and Kyoto Encyclopedia of Genes and Genomes (KEGG) pathway enrichment analysis

KEGG pathways and GO enrichment analysis was conducted to explore the potential functions of the essential protein targets of mahogany metabolites with the Database for Annotation, Visualization, and Integrated Discovery (DAVID). GO analysis involved three categories: biological process (BP), cellular component (CC), and molecular function (MF). $P < 0.05$ was set as the thresholds for significant enrichment analysis.²⁰

Protein-protein interaction (PPI) network of predictive biomarkers and hub gene construction

The PPI data were obtained from the Search Tool for the Retrieval of Interacting Genes (STRING) database (<https://string-db.org>), which can predict interactions among proteins. The prediction method of this database was derived from experiments, databases, and text mining of the neighborhood, gene fusion, co-occurrence, and co-expression. In the present study, PPIs with combined scores >0.4 were selected for further research. The Cytoscape software (<http://www.cytoscape.org>) was used to establish a PPI network. In addition, the Cytohubba was applied to analyze the PPI network to obtain the top 20 nodes that were considered hub genes according to the degree value.²¹

RESULTS

Predicted compounds of mahogany showed inhibitory activity against HMG-CoA reductase

The study of mahogany metabolites on predicting HMGCR inhibition was performed using the KNIME software by predicting the inhibitory activity of one or more compounds at once against the targeted protein (mahogany-stated inhibition of HMGCR). The prediction model was constructed with the KNIME software by adapting the Teach-Open CADD pipeline.¹⁸ The dataset for constructing the prediction model was a dataset of HMGCR inhibitory activity, which is provided in ChEMBL with ID dataset ChEMBL407. Based on the MACCS fingerprint of the inhibitor compounds from the dataset, ML had mapped all compound fingerprints to prepare a predictive model of the inhibitory activity from the targeted protein.²² The HMGCR inhibitory compound data set was split into active and inactive compounds and used to train ML classifiers based on two ML algorithms: Random Forest (RF) and Artificial Neural Network (ANN). Validation of the prediction models from two different MLs suggested that all prediction models had an overall accuracy value $>90\%$ (RF 92.07% and ANN 90.24%) and ROC curve p scores >0.75 (RF 0.932 dan ANN 0.879). These results indicated that the prediction model was valid and could predict the inhibitory activity of compounds in mahogany.²³

The results of the inhibitory activity prediction revealed that potential compounds of mahogany metabolites inhibited HMGCR. Based on the prediction model under ML algorithms, ANN showed 5 compounds, namely, β -sitosterol, swietemacrophyllanin, 7-hydroxy-2-(4-hydroxy-3-methoxyphenyl)-chroman-4-on (7HMC), scopoletin, and stigmaterol, which were predicted to possess inhibitory

activity against HMGCR based on the number of predictive values being 1.00 and 0.99. Analyzing the RF algorithm presented the same result as that with ANN, with the highest predictive value of 0.9 for scopoletin (Table I). These inhibitory activities were predicted based on the likeness of structure and inhibitory activity with those of known inhibitor compounds processed by the RF and ANN algorithms.

Targeted genes prediction of mahogany potential compounds

Predictive target genes of each potential mahogany metabolites using databases SwissTargetPrediction obtained from the default settings. We obtained 100 targets for each compound (Fig. 1). A Venn diagram was used to determine all compounds' total targeted genes to ensure no duplication of the targets. A total of 294 genes were known predicted as the target of the 5 potential compounds (Table II and Table III).

KEGG pathway and GO enrichment analysis

A total of 294 common targets were subjected to the DAVID v6.8 database for gene enrichments. GO and KEGG gene enrichment results were put in order according to the percentage of genes. The top 5 GO results in the KEGG pathway, biological process, cellular component, and molecular function were recorded.

KEGG pathway enrichment analysis revealed that the genes were regulated in the cancer signaling pathways, PI3K-Akt, neuroactive ligand-receptor interaction, proteoglycan in cancer, and viral carcinogenesis pathway (Table IV). The results for GO analysis were evaluated through the related term option of the DAVID database. According to biological process results, protein phosphorylation, signal transduction, response to drug, oxidation-reduction process, and positive regulation of transcription from RNA polymerase II promoter showed higher targeted numbers in the count. Molecular function results with higher targeted numbers included protein binding, ATP binding, protein kinase activity, protein serine/threonine kinase activity, and zinc ion binding, which were found to be related to at least one of the KEGG pathways such as the cancer signaling pathways, PI3K-Akt, neuroactive ligand-receptor interaction, proteoglycan in cancer, and viral carcinogenesis pathway. Moreover, based on the analysis, most of the genes were present in the cellular components of the plasma membrane, nucleus, cytoplasm, and integral component of membrane.

PPI network construction and hub gene selection

Construction of the PPIs network among the targeted genes of mahogany compounds and identification of the most significant modules using the online tool STRING with a cutoff score of ≥ 0.4 . A total of 294 genes were constructed to

the PPI network complex containing 294 nodes and 3150 edges, with an average node degree of 22.2, an average local clustering coefficient of 0.465, and a PPI enrichment p-value of $<1.0e-16$ (Fig. 2a). Using the cytoHubba plugin Cytoscape, we detected the top 20 targeted genes with the uppermost degree score, including AKT1, MAPK3, EGFR, SRC, MAPK1, VEGFA, SKP90AA1, ESR1, PTGS2, MTOR, PIK3CA, APP, MMP9, MAPK14, AR, ERBB2, MDM2, KDR, BCL2L1, and STAT1 (Fig 2b, Table V).

DISCUSSION

The present study investigated the potency of mahogany compounds and their molecular targets and signaling mechanism as an alternative treatment for preventing dyslipidemia during menopause through bioinformatics analyses. This study was conducted to determine which compounds were responsible for the anti-dyslipidemic effect of mahogany. Moreover, the predictive targeted genes of the compounds showed inhibit activity against HMGCR under hyperlipidemia conditions. It uses data on HMGCR inhibitor compounds that have been studied, which is then used to perform ML on the fingerprint pattern of the inhibitor compounds for the prediction of compounds in mahogany with inhibitory activity against HMGCR.¹⁸ Past analysis suggests β -sitosterol, swietemachrophyllanin, 7-HMC, scopoletin, and stigmasterol as compounds that can be suspected to be responsible for the anti-dyslipidemia effect of mahogany through the inhibition of HMGCR (Table I). Targeted genes' exploration predicted 294 genes is the target of the 5 mahogany potential metabolites. Twenty potential hub genes including MAPK, AKT1, PI3K, MTOR, and ER1, and others were screened as effective targets of mahogany compounds (Fig. 2, Table V).

Past studies have shown that the ethanolic extract of the seeds, leaves, and bark of mahogany tree possesses hypolipidemic activity and can reduce the HMGCR activity.²⁴ HMGCR is a rate-limiting enzyme of cholesterol biosynthesis. HMGCR inhibitors (ex, statins) are currently the mainstay of treatment for dyslipidemia. Nevertheless, during the menopause condition, treatment with only a single statin cannot alleviate the other menopausal syndromes.²⁵ Under physiological conditions, HMGCR activity is regulated by multiple mechanisms. At the transcriptional level, the expression of the HMGCR gene is regulated by the sterol regulatory element-binding proteins (SREBP).²⁶ SREBPs can be mainly categorized as SREBP1 and SREBP2, where every subunit plays an essential role in lipid and cholesterol biosynthesis. SREBP1 activates mostly those genes that are related to fatty acid biosynthesis or carbohydrate metabolism, while SREBP2 primarily activates cholesterol synthesis-related genes.²⁷ SREBP2 was also predicted as a

Table I: The predicted value of HMG-CoA reductase inhibitory activity of mahogany metabolites

No	Compound	Prediction value (1.0)	
		ANN	RF
1	β -sitosterol	0.99	0.84
2	Swietemacrophyllanin	1.00	0.79
3	(7HMC)	1.00	0.86
4	Scopoletin	1.00	0.9
5	Stigmasterol	1.00	0.83

Table II: Prediction 100 protein target of a potential mahogany compound through Swiss Target Prediction

No	B-sitosterol	Swietemacphyllanin	7HMC	Stigmasterol	Scopoletin
1	AR	PGF	CYP1B1	AR	CA7
2	HMGCR	VEGFA	CYP19A1	NPC1L1	CA12
3	CYP51A1	MMP2	TAS2R31	HMGCR	CA9
4	NPC1L1	MMP9	CA7	CYP51A1	CA13
5	NR1H3	SQLE	CA12	CYP19A1	CA1
6	CYP19A1	BACE1	CA4	NR1H3	CA14
7	CYP17A1	CA5B	ADORA1	CYP17A1	CA4
8	RORC	MMP13	ADORA3	RORC	EGFR
9	ESR1	MMP12	ESR1	ESR1	CA5A
10	ESR2	PTGS1	ESR2	ESR2	XDH
11	SREBF2	CA2	MAOB	SHBG	CA6
12	SHBG	CA1	HSD17B1	SREBF2	CA2
13	SLC6A2	DNM1	MMP13	ACHE	SRD5A1
14	CYP2C19	CA4	ABCG2	CYP2C19	CBR1
15	RORA	CA7	ABCC1	PTPN1	CDK2 CCNA1 CCNA2
16	PTPN1	CA12	SHBG	SLC6A2	MAOA
17	BCHE	CA9	CBR1	BCHE	ESR2
18	SERPINA6	CYP19A1	MMP12	RORA	ALOX5
19	SLC6A4	HIF1A	PTGS1	SERPINA6	CCND1 CDK4
20	CHRM2	BCL2	CA2	SLC6A4	FLT4
21	VDR	MMP14	CA1	CHRM2	INSR
22	ACHE	SYK	CA6	G6PD	PTK2
23	G6PD	MAPT	CA5A	VDR	PLK1
24	NR1H2	TERT	CA3	NR1H2	TEK
25	GLRA1	PGD	APP	HSD11B1	MAP3K8
26	CES2	ST3GAL3	KLK1	PTGER1	HSPA1A
27	PTGER1	FUT7	KLK2	PTGER2	NUAK1
28	PTGER2	FUT4	PLA2G1B	CDC25A	FGR
29	HSD11B1	PDK1	ACHE	GLRA1	CA5B
30	PTGES	ABCB1	CHRNA7	CES2	AKR1C1
31	CDC25A	PIK3CA PIK3R1	BACE1	PTGES	DAO
32	PPARA	PIK3CD PIK3R1	SRC	PPARA	GSK3B
33	PPARD	PIK3R1 PIK3CB	SGK1	PPARD	KCNA3
34	DHCR7	MTOR	ERN1	SQLE	PTGS2
35	SQLE	PIK3CG	RP56KB1	DHCR7	GSR
36	PTPN6	PIK3CA	AURKA	NR1I3	HSD17B3
37	NR1I3	MET	POLB	PTPN6	SRC
38	FDFT1	CA3	CA9	NR3C1	KDR
39	SIGMAR1	CA6	CA13	CDC25B	ACHE
40	NOS2	CA5A	CA5B	NOS2	CYP1A2
41	NR3C1	ALPL	GRM2	HSD11B2	NAT1
42	PPARG	PLAA	PLA2G5	TBXAS1	MAOB
43	CDC25B	FCER2	EDNRA	PPARG	PTPN1
44	UGT2B7	TYMP	MET	UGT2B7	ESR1
45	HSD11B2	PRKDC	MMP2	POLB	MB
46	POLB	MAPK3	NOX4	PREP	PARP1
47	PREP	MAPK1	PLG	SIGMAR1	KCNMA1
48	PTGER4	PCNA	MMP3	PTGER4	ERBB2
49	IDO1	POLB	MMP7	IDO1	SQLE
50	DRD2	FBP1	PPARG	MDM4	BACE1
51	TBXAS1	MMP7	MMP9	DRD2	MET
52	ATP12A	MMP8	SLC5A2	MDM2	COMT
53	MDM4	GABRA1 GABRB2 GABRG2	BCL2	ATP12A	GPR35
54	MDM2	PLA2G2A	CDK2 CCNA1 CCNA2	MGLL	CDK9 CCNT1
55	PTGIR	PLA2G5	DNM1	PTGIR	AKR1C3
56	DHCR7 EBP	PLA2G10	DYRK1A	DHCR7 EBP	ALPG
57	FABP4	GAK	RXRA	FABP4	PLAA
58	TERT	ERN1	BCHE	FABP3	AKR1B1
59	FABP3	HDAC2	HSD17B2	FABP5	AURKA
60	FABP5	P2RX3	CHEK1	FABP1	CHRM1
61	FABP1	CYP1B1	CDK2	BACE2	AOC3
62	ADORA3	PIM1	CDC7	ADORA3	AURKB
63	MAPK3	PIM2	KDR	MAPK3	CISD1
64	PTPN11	PIM3	BRAF	PTPN11	AKT1
65	AKR1B10	EDNRA	ODC1	AKR1B10	PLEC
66	PRKCG	KLK1	BCL2L1	CCR1	CSNK1A1
67	PRKCD	KLK2	CLK1	GABBR1	CSNK1D
68	PRKCB	ADAM17	DYRK1B	BACE1	HMGCR
69	PRKCE	NCOR2 HDAC3	DNMT1	PTPRF	ALPL

cont..... pg 70

cont from..... pg 69

Table II: Prediction 100 protein target of a potential mahogany compound through Swiss Target Prediction

No	B-sitosterol	Swietemacphyllanin	7HMC	Stigmasterol	Scopoletin
70	PRKCQ	HDAC5	PGD	PLA2G1B	BRAF
71	PTPRF	HDAC7	ST3GAL3	ACP1	ALDH5A1
72	PLA2G1B	PIK3CB	FUT7	SCD	ABAT
73	ACP1	HDAC4	FUT4	MAPK14	CSNK2A1
74	IGF1R	HDAC10	STAT1	GRM2	APEX1
75	SRC	HDAC3	SQLE	ACACB	CXCR1
76	KDR	PLG	MMP8	MTNR1A	PIK3CG
77	ALK	PLAU	CDK4	MTNR1B	CLK1
78	SCD	PLA2G7	CES1	TOP2A	DYRK1B
79	MGLL	CHRM1	SERPINE1	IGF1R	IGF1R
80	BACE1	TOP1	ABCB1	SRC	PTPRC
81	CCR1	CDK2	RPS6KA3	KDR	GRK6
82	TOP2A	CDK1	CHEK2	ALK	TNNC1 TNNT2 TNNI3
83	GABBR1	HSP90AA1	RPS6KA1	PRKCG	EPHB4
84	BACE2	KCNH2	WEE1	PRKCD	PDGFRB
85	MAPK14	JAK3	BMP1	PRKCB	PLK4
86	F11	JAK1	OPRK1	PRKCE	LYN
87	PTGFR	SCN9A	DUSP3	PRKCQ	PNP
88	PTGER3	CCNE2 CDK2 CCNE1	HDAC5	PTPN2	TAAR1
89	PTGDR	LCK	HDAC7	KCNA5	PIM3
90	TOP1	ITK	HDAC4	TACR1	HTR2B
91	HIF1A	JAK2	PNP	PTGFR	TERT
92	ACACB	TXK	YWHAG	PTGER3	CA3
93	PRKCH	F11	CES2	PTGDR	JAK1
94	PTPN2	PNMT	AKR1C3	AGTR1	JAK2
95	TACR1	KDR	TYMS	CNR1	TYK2
96	MTNR1A	FGFR1	ECE1	TOP1	F2
97	MTNR1B	HSD17B2	MMP14	HIF1A	CHEK1
98	NPY5R	HSD17B3	GABRA1 GABRB2 GABRG2	F11	WEE1
99	SLC22A6	ESR1	PTPN1	HTR2B	ADRA2A
100	MAP3K14	ESR2	TERT	AVPR1A	ADRA2C

Table III: The total of 294 genes were known predicted as the target of the 5 potential compounds

No	Genes	No	Genes	No	Genes
1	<i>FDFT1</i>	101	<i>NAT1</i>	201	<i>CDC25A</i>
2	<i>PRKCH</i>	102	<i>MB</i>	202	<i>PPARA</i>
3	<i>NPY5R</i>	103	<i>PARP1</i>	203	<i>PPARD</i>
4	<i>SLC22A6</i>	104	<i>KCNMA1</i>	204	<i>DHCR7</i>
5	<i>MAP3K14</i>	105	<i>ERBB2</i>	205	<i>PTPN6</i>
6	<i>PGF</i>	106	<i>COMT</i>	206	<i>NR1I3</i>
7	<i>VEGFA</i>	107	<i>GPR35</i>	207	<i>SIGMAR1</i>
8	<i>SYK</i>	108	<i>CDK9 CCNT1</i>	208	<i>NOS2</i>
9	<i>MAPT</i>	109	<i>ALPG</i>	209	<i>NR3C1</i>
10	<i>PDK1</i>	110	<i>AKR1B1</i>	210	<i>CDC25B</i>
11	<i>PIK3CA PIK3R1</i>	111	<i>AOC3</i>	211	<i>UGT2B7</i>
12	<i>PIK3CD PIK3R1</i>	112	<i>AURKB</i>	212	<i>HSD11B2</i>
13	<i>PIK3R1 PIK3CB</i>	113	<i>CISD1</i>	213	<i>PREP</i>
14	<i>MTOR</i>	114	<i>AKT1</i>	214	<i>PTGER4</i>
15	<i>PIK3CA</i>	115	<i>PLEC</i>	215	<i>IDO1</i>
16	<i>FCER2</i>	116	<i>CSNK1A1</i>	216	<i>DRD2</i>
17	<i>TYMP</i>	117	<i>CSNK1D</i>	217	<i>TBXAS1</i>
18	<i>PRKDC</i>	118	<i>ALDH5A1</i>	218	<i>ATP12A</i>
19	<i>MAPK1</i>	119	<i>ABAT</i>	219	<i>MDM4</i>
20	<i>PCNA</i>	120	<i>CSNK2A1</i>	220	<i>MDM2</i>
21	<i>FBP1</i>	121	<i>APEX1</i>	221	<i>PTGIR</i>
22	<i>PLA2G2A</i>	122	<i>CXCR1</i>	222	<i>DHCR7 EBP</i>
23	<i>PLA2G10</i>	123	<i>PTPRC</i>	223	<i>FABP4</i>
24	<i>GAK</i>	124	<i>GRK6</i>	224	<i>FABP3</i>
25	<i>HDAC2</i>	125	<i>TNNC1 TNNT2 TNNI3</i>	225	<i>FABP5</i>
26	<i>P2RX3</i>	126	<i>EPHB4</i>	226	<i>FABP1</i>
27	<i>PIM1</i>	127	<i>PDGFRB</i>	227	<i>PTPN11</i>
28	<i>PIM2</i>	128	<i>PLK4</i>	228	<i>AKR1B10</i>
29	<i>ADAM17</i>	129	<i>LYN</i>	229	<i>PRKCG</i>
30	<i>NCOR2 HDAC3</i>	130	<i>TAAR1</i>	230	<i>PRKCD</i>
31	<i>PIK3CB</i>	131	<i>TYK2</i>	231	<i>PRKCB</i>
32	<i>HDAC10</i>	132	<i>F2</i>	232	<i>PRKCE</i>

cont..... pg 71

cont from..... pg 70

Table III: The total of 294 genes were known predicted as the target of the 5 potential compounds

No	Genes	No	Genes	No	Genes
33	HDAC3	133	ADRA2A	233	PRKCQ
34	PLAU	134	ADRA2C	234	PTPRF
35	PLA2G7	135	KCNA5	235	ACP1
36	CDK1	136	AGTR1	236	ALK
37	HSP90AA1	137	CNR1	237	SCD
38	KCNH2	138	AVPR1A	238	MGLL
39	JAK3	139	MMP2	239	CCR1
40	SCN9A	140	MMP9	240	TOP2A
41	CCNE2 CDK2 CCNE1	141	MMP13	241	GABBR1
42	LCK	142	MMP12	242	BACE2
43	ITK	143	PTGS1	243	MAPK14
44	TXK	144	DNM1	244	PTGFR
45	PNMT	145	BCL2	245	PTGER3
46	FGFR1	146	MMP14	246	PTGDR
47	TAS2R31	147	PGD	247	ACACB
48	ADORA1	148	ST3GAL3	248	PTPN2
49	HSD17B1	149	FUT7	249	TACR1
50	ABCG2	150	FUT4	250	MTNR1A
51	ABCC1	151	ABCB1	251	MTNR1B
52	APP	152	MMP7	252	PIK3CG
53	CHRNA7	153	MMP8	253	ALPL
54	SGK1	154	GABRA1 GABRB2	254	PLAA
			GABRG2		
55	RPS6KB1	155	PLA2G5	255	PIM3
56	NOX4	156	ERN1	256	CHRM1
57	MMP3	157	CYP1B1	257	JAK1
58	SLC5A2	158	EDNRA	258	JAK2
59	DYRK1A	159	KLK1	259	HSD17B3
60	RXRA	160	KLK2	260	GRM2
61	CDC7	161	HDAC5	261	SHBG
62	ODC1	162	HDAC7	262	BCHE
63	BCL2L1	163	HDAC4	263	CES2
64	DNMT1	164	PLG	264	PPARG
65	STAT1	165	CDK2	265	ADORA3
66	CDK4	166	HSD17B2	266	PLA2G1B
67	CES1	167	MAOB	267	HMGCR
68	SERPINE1	168	CBR1	268	IGF1R
69	RPS6KA3	169	AURKA	269	MAPK3
70	CHEK2	170	CA13	270	F11
71	RPS6KA1	171	CDK2 CCNA1 CCNA2	271	TOP1
72	BMP1	172	CHEK1	272	HIF1A
73	OPRK1	173	BRAF	273	CYP19A1
74	DUSP3	174	CLK1	274	POLB
75	YWHAG	175	DYRK1B	275	TERT
76	TYMS	176	WEE1	276	CA5B
77	ECE1	177	PNP	277	CA2
78	CA14	178	AKR1C3	278	CA1
79	EGFR	179	HTR2B	279	CA4
80	XDH	180	AR	280	CA7
81	SRD5A1	181	CYP51A1	281	CA12
82	MAOA	182	NPC1L1	282	CA9
83	ALOX5	183	NR1H3	283	MET
84	CCND1 CDK4	184	CYP17A1	284	CA3
85	FLT4	185	RORC	285	CA6
86	INSR	186	SREBF2	286	CA5A
87	PTK2	187	SLC6A2	287	PTPN1
88	PLK1	188	CYP2C19	288	ACHE
89	TEK	189	RORA	289	SRC
90	MAP3K8	190	SERPINA6	290	ESR1
91	HSPA1A	191	SLC6A4	291	ESR2
92	NUAK1	192	CHRM2	292	SQLE
93	FGR	193	VDR	293	KDR
94	AKR1C1	194	G6PD	294	BACE1
95	DAO	195	NR1H2		
96	GSK3B	196	GLRA1		
97	KCNA3	197	PTGER1		
98	PTGS2	198	PTGER2		
99	GSR	199	HSD11B1		
100	CYP1A2	200	PTGES		

Table IV: Top five results of KEGG pathway dan Gene Ontology enrichment analysis of the potential targeted genes using DAVID v6.8.

Term	Count	P-Value	Genes
hsa05200: Pathways in cancer	49	3.21162E-13	<i>GSK3B, PIK3CD, PIK3CB, PIK3CG, IGF1R, EDNRA, CCND1, AKT1, JAK1, PDGFRB, PRKCG, HSP90AA1, PRKCB, MMP2, MMP9, PGF, AR, PIK3CA, CCNE2, CCNE1, AGTR1, PPARG, MET, PPAR, PTGER4, HDAC2, PTGER1, PTGER2, PTGER3, PIK3R1, PTGS2, HIF1A, EGFR, RXRA, ERBB2, MAPK1, MAPK3, NOS2, STAT1, BRAF, MTOR, PTK2, VEGFA, CDK4, CDK2, BCL2, MDM2, FGFR1, BCL2L1</i>
hsa04151:PI3K-Akt signaling pathway	41	2.03355E-10	<i>CHRM2, GSK3B, CHRM1, FLT4, PIK3CD, PIK3CB, PIK3R1, EGFR, PIK3CG, IGF1R, RXRA, CCND1, KDR, AKT1, MAPK1, JAK2, JAK3, YWHAG, JAK1, MAPK3, PDGFRB, HSP90AA1, SYK, INSR, MTOR, PGF, PTK2, VEGFA, PIK3CA, CCNE2, RPS6KB1, CCNE1, CDK4, CDK2, BCL2, MDM2, TEK, SGK1, MET, FGFR1, BCL2L1</i>
hsa04080: Neuroactive ligand-receptor interaction	37	7.16148E-11	<i>PTGER4, CHRM2, GABRB2, PTGFR, CHRM1, PTGER1, PTGER2, CHRNA7, PTGER3, HTR2B, PLG, NR3C1, GRM2, GLRA1, EDNRA, CNR1, ADORA3, ADORA1, DRD2, PTGDR, GABRA1, PTGIR, GABBR1, NPY5R, GPR35, OPRK1, TACR1, AVPR1A, ADRA2C, F2, TAAR1, GABRG2, ADRA2A, MTNR1A, P2RX3, MTNR1B, AGTR1</i>
hsa05205: Proteoglycans in cancer	32	1.78808E-11	<i>SRC, PIK3CD, PIK3CB, PIK3R1, HIF1A, EGFR, PIK3CG, IGF1R, CCND1, PLAU, ERBB2, KDR, AKT1, MAPK1, MAPK3, PRKCG, PRKCB, MMP2, PTPN11, BRAF, MAPK14, MMP9, ESR1, MTOR, PTK2, VEGFA, PIK3CA, RPS6KB1, MDM2, PTPN6, MET, FGFR1</i>
hsa05203: Viral carcinogenesis	30	7.95804E-10	<i>HDAC4, HDAC5, HDAC2, HDAC3, HDAC10, SRC, PIK3CD, PIK3CB, PIK3R1, PIK3CG, HDAC7, POLB, CCND1, CHEK1, MAPK1, JAK3, YWHAG, JAK1, MAPK3, LYN, SYK, CCNA2, CCNA1, PIK3CA, CCNE2, CCNE1, CDK4, CDK2, CDK1, MDM2</i>

Molecular function

Term	Count	P-Value	Genes
GO:0005515~protein binding	199	2.66061E-07	<i>APP, HDAC10, SERPINE1, PREP, RPS6KA3, EDNRA, CHEK2, RPS6KA1, CHEK1, KDR, AKT1, EPHB4, PDK1, PTGDR, CSNK2A1, PRKCB, PRKCE, PRKCD, CSNK1D, GABRG2, AR, AGTR1, PRKCQ, SLC22A6, ABCB1, PRKDC, TXK, PIK3R1, HIF1A, NUAK1, TERT, CCR1, LYN, PLK4, INSR, PLK1, CDC7, BRAF, PTK2, AKR1B10, NOX4, TOP2A, ACHE, ITK, SLC6A2, SLC6A4, JAK2, JAK3, JAK1, PARP1, SYK, TNNC1, AVPR1A, TYK2, TACR1, F2, SREBF2, GAK, BACE1, NCOR2, FCER2, MMP14, TNNT2, KCNMA1, PPARG, MAPT, SGK1, PPARA, PPAR, PTGER4, PCNA, ODC1, KCNA5, PTGS2, EGFR, GLRA1, RXRA, ALOX5, AOC3, GABBR1, STAT1, CSNK1A1, AKR1C1, NR1H2, F11, NR1H3, VEGFA, FABP1, FABP3, FABP5, APEX1, HSPA1A, CCNT1, RORC, RORA, COMT, NR3C1, IGF1R, CCND1, PLAU, ADORA1, PIM1, MAP3K8, PIM3, PIM2, PDGFRB, KCNH2, G6PD, DYRK1A, DYRK1B, PGF, CDC25A, CDC25B, ERN1, ADAM17, MTNR1A, CCNE2, CCNE1, MTNR1B, PLAA, ABCG2, DNMT1, ACACB, NPC1L1, GRK6, DRD2, VDR, ESR1, ESR2, CDK9, CLK1, DAO, BMP1, PTPRC, CDK4, CDK2, BCL2, MDM2, CDK1, ALPL, MDM4, MAP3K14, BCL2L1, FGFR1, ALK, GSK3B, FLT4, PIK3CD, ECE1, PIK3CB, PIK3CG, POLB, GRM2, CA1, CA2, CA4, ACP1, YWHAG, HSP90AA1, MMP2, MMP3, ADRA2C, MMP9, ADRA2A, DNMT1, FGR, CCNA2, CCNA1, PIK3CA, LCK, TOP1, MET, FBP1, PLEC, HDAC4, HDAC5, HDAC2, HDAC3, SRC, PLG, HMGR, AURKB, AURKA, HDAC7, ERBB2, MAPK1, TNNT3, MAPK3, PTPN1, NOS2, OPRK1, PTPN11, MAPK14, MTOR, WEE1, RPS6KB1, PTPN6, TEK, PTPN2</i>
GO:0005524~ATP binding	83	2.15845E-21	<i>ALK, TOP2A, GSK3B, ITK, FLT4, PIK3CD, PIK3CB, ATP12A, PIK3CG, IGF1R, RPS6KA3, CHEK2, RPS6KA1, CHEK1, PIM1, KDR, AKT1, PIM3, MAP3K8, PIM2, JAK2, JAK3, EPHB4, JAK1, PDK1, PDGFRB, PRKCG, ABCB1, HSP90AA1, PRKCH, CSNK2A1, SYK, PRKCB, PRKCE, PRKCD, DYRK1A, DYRK1B, CSNK1D, TYK2, GAK, ERN1, FGR, PIK3CA, LCK, PRKCQ, SGK1, MET, ABCG2, ABCB1, SRC, PRKDC, TXK, ACACB, EGFR, AURKB, AURKA, NUAK1, ERBB2, GRK6, MAPK1, MAPK3, LYN, PLK4, CSNK1A1, INSR, PLK1, BRAF, CDC7, MAPK14, MTOR, PTK2, CDK9, CLK1, WEE1, P2RX3, RPS6KB1, CDK4, CDK2, CDK1, TEK, MAP3K14, FGFR1, HSPA1A</i>
GO:0004672~protein kinase activity	51	1.5312E-30	<i>GSK3B, PIK3CG, RPS6KA3, CCND1, CHEK2, RPS6KA1, CHEK1, AKT1, PIM3, MAP3K8, PIM2, JAK2, PDK1, PRKCG, PRKCH, CSNK2A1, SYK, PRKCB, PRKCE, PRKCD, DYRK1A, DYRK1B, CSNK1D, TYK2, GAK, PRKCQ, MET, SRC, PRKDC, TXK, EGFR, AURKB, AURKA, NUAK1, ERBB2, CSNK1A1, PLK1, BRAF, CDC7, MAPK14, MTOR, PTK2, CDK9, CLK1, WEE1, RPS6KB1, CDK4, CDK2, CDK1, TEK, MAP3K14</i>

cont from..... pg 72

Table IV: Top five results of KEGG pathway dan Gene Ontology enrichment analysis of the potential targeted genes using DAVID v6.8.

GO:0004674~protein serine/threonine kinase activity	45	9.24148E-24	GSK3B, CCNT1, PRKDC, PIK3CG, AURKB, AURKA, RPS6KA3, NUAK1, CHEK2, CHEK1, RPS6KA1, PIM1, AKT1, MAPK1, PIM3, MAP3K8, PIM2, MAPK3, PLK4, PRKCH, SYK, CSNK2A1, PRKCB, CSNK1A1, PRKCE, PRKCD, PLK1, DYRK1A, DYRK1B, BRAF, CSNK1D, CDC7, MAPK14, MTOR, CDK9, GAK, ERN1, CLK1, PIK3CA, CDK4, CDK2, CDK1, PRKCQ, SGK1, MAP3K14.
GO:0008270~zinc ion binding	43	8.45694E-06	HDAC4, DNMT1, NR1I3, RORC, RORA, NR3C1, GLRA1, CA1, RXRA, CA5B, CA3, CA2, CA5A, CA4, CA7, CA6, CA9, CA13, CA12, PRKCG, PTPN1, MMP7, PARP1, PRKCB, VDR, NR1H2, MMP2, MMP3, NR1H3, MMP8, MMP9, ESR1, ESR2, MMP12, AR, MMP14, BMP1, MMP13, MDM2, PPARG, MDM4, PPARA, PPARD.

Biological process

Term	Count	P-Value	Genes
GO:0006468~protein phosphorylation	56	2.74809E-30	APP, GSK3B, CCNT1, PIK3CD, PIK3CG, RPS6KA3, CCND1, CHEK2, RPS6KA1, PIM1, AKT1, PIM3, MAP3K8, PIM2, JAK2, JAK3, JAK1, PDK1, PRKCG, PRKCH, CSNK2A1, SYK, PRKCB, PRKCE, PRKCD, DYRK1A, DYRK1B, CSNK1D, TYK2, CDC25B, GAK, ERN1, FGR, PIK3CA, CCNE1, LCK, SGK1, TXK, PIK3R1, AURKB, AURKA, NUAK1, ERBB2, GRK6, MAPK1, MAPK3, LYN, PLK4, CSNK1A1, PLK1, BRAF, MTOR, CDK9, RPS6KB1, CDK4, FGFR1.
GO:0007165~signal transduction	51	3.74565E-09	ALK, ITK, CHRM1, PIK3CD, PIK3CB, NR3C1, IGF1R, RPS6KA3, EDNRA, PLAU, RPS6KA1, ADORA1, AKT1, JAK2, PDGFRB, HSP90AA1, PRKCH, CSNK2A1, PRKCB, PRKCE, PRKCD, CSNK1D, ADRA2A, PGF, AR, PLAA, PPARG, MET, PTGES, SRC, PLA2G1B, NR1I3, CHRNA7, PIK3R1, HIF1A, EGFR, EBP, ERBB2, GRK6, MAPK1, LYN, CSNK1A1, VDR, MAPK14, ESR1, MTOR, ESR2, P2RX3, RPS6KB1, CDK4, TEK.
GO:0042493~response to drug	40	1.44432E-22	HDAC4, HDAC5, HDAC2, ABCB1, MAOB, SRC, HTR2B, ABAT, TYMS, COMT, PTGS2, SLC6A2, ACACB, SLC6A4, HSD11B2, PNP, CCND1, NPC1L1, CA9, DRD2, LYN, BCHE, ABCC1, HSP90AA1, STAT1, SRD5A1, PGF, CDK9, ADAM17, FABP3, RPS6KB1, LCK, CDK4, APEX1, BCL2, CDK1, MDM2, PPARG, TOP1, ABCG2.
GO:0055114~oxidation-reduction process	38	2.42738E-11	MAOB, MAOA, HSD17B3, AKR1B1, HMGCR, CYP2C19, PTGS2, CYP19A1, PTGS1, CYP17A1, HSD11B1, HSD11B2, HSD17B1, ALOX5, HSD17B2, CYP1B1, XDH, FDF1, AOC3, CBR1, G6PD, NOS2, SRD5A1, AKR1C1, GSR, CYP51A1, AKR1C3, PGD, SQLE, DAO, AKR1B10, SCD, APEX1, TBXAS1, CYP1A2, NOX4, DHCR7, IDO1.
GO:0045944~positive regulation of transcription from RNA polymerase II promoter	38	1.10342E-05	HDAC4, TOP2A, HDAC5, APP, GSK3B, HDAC2, HDAC3, CCNT1, PLA2G1B, PRKDC, NR1I3, TXK, SERPINE1, RORA, PIK3R1, NR3C1, HIF1A, EGFR, RPS6KA3, RXRA, RPS6KA1, AKT1, DRD2, MAPK3, PARP1, STAT1, VDR, NR1H2, NR1H3, MAPK14, ESR1, SREBF2, VEGFA, CDK9, AR, PPARG, PPARA, MET.

Cell component

Term	Count	P-Value	Genes
GO:0005886~plasma membrane	123	8.03158E-13	CHRM2, APP, CHRM1, SERPINE1, COMT, ATP12A, IGF1R, EDNRA, PLAU, ADORA3, ADORA1, PIM1, KDR, AKT1, EPHB4, CA14, PTGDR, PDGFRB, KCNH2, PRKCG, PRKCH, CSNK2A1, PRKCB, PRKCE, PRKCD, CSNK1D, TAAR1, GABRG2, AR, MTNR1A, ADAM17, MTNR1B, AGTR1, PRKCQ, ABCG2, PTGFR, SLC22A6, ABCB1, CHRNA7, PIK3R1, PLA2G5, SLC5A2, TERT, NPC1L1, GRK6, DRD2, CCR1, LYN, TAS2R31, INSR, BRAF, ESR1, PTK2, PTPRC, MDM2, ALPL, FGFR1, GABRB2, ACHE, GSK3B, FLT4, HTR2B, PIK3CD, ECE1, PIK3CB, SLC6A2, PTPRF, PIK3CG, SLC6A4, GRM2, CA2, CA4, CA9, ABCC1, PTGIR, HSP90AA1, NPY5R, SYK, MMP2, AVPR1A, TACR1, F2, ADRA2C, ADRA2A, DNMT1, BACE1, FGR, FCER2, MMP14, PIK3CA, LCK, KCNMA1, MAPT, SGK1, MET, MGLL, PLEC, PTGER4, HDAC3, SRC, PTGER1, PTGER2, PTGER3, KCNA3, KCNA5, PLG, EGFR, GLRA1, CXCR1, CNR1, ERBB2, CA12, AOC3, PTPN1, GABRA1, GABBR1, CYP51A1, F11, PLA2G2A, OPRK1, P2RX3, TEK, PTPN2
GO:0005829~cytosol	118	4.75122E-18	PNMT, APP, COMT, RPS6KA3, PNP, CCND1, RPS6KA1, CHEK1, AKT1, MAP3K8, EPHB4, CA13, PRKCG, G6PD, PRKCH, CSNK2A1, PRKCB, PRKCE, PRKCD, CSNK1D, PGD, CDC25A, CDC25B, AR, CCNE2, CCNE1, PRKCQ, IDO1, CES1, PRKDC, PIK3R1, HIF1A, ACACB, LYN, PLK4, PLK1, BRAF, PTK2, DAO, AKR1B10, NAT1, CDK4, CDK2, BCL2, MDM2, CDK1, MAP3K14, BCL2L1, FGFR1, GABRB2, GSK3B, ITK, PIK3CD, AKR1B1, PIK3CB, PIK3CG, SLC6A4, CA1, CA3, CA2, CA7, CA6, JAK2, JAK3, YWHAG, JAK1, CBR1, PTGIR,

cont..... pg 74

cont from..... pg 73

Table IV: Top five results of KEGG pathway dan Gene Ontology enrichment analysis of the potential targeted genes using DAVID v6.8.

			<i>HSP90AA1, DUSP3, SYK, TNNC1, TYK2, SREBF2, GAK, FGR, CCNA1, PIK3CA, LCK, TNNT2, PPARG, MAPT, SGK1, FBP1, MGLL, PLEC, HDAC4, HDAC3, SRC, NR1I3, ODC1, TYMS, AURKB, TYMP, AURKA, HSD17B1, ALOX5, MAPK1, TNNI3, XDH, MAPK3, PTPN1, NOS2, STAT1, CSNK1A1, AKR1C1, GSR, AKR1C3, PTPN11, MAPK14, MTOR, FABP1, FABP3, FABP4, RPS6KB1, FABP5, PTPN6, HSPA1A</i>
GO:0005634~nucleus	110	0.006034134	<i>CCNT1, HDAC10, PREP, RORC, RORA, NR3C1, RPS6KA3, PNP, CCND1, RPS6KA1, CHEK1, PIM1, KDR, AKT1, PDGFRB, PRKCG, G6PD, CSNK2A1, PRKCB, PRKCE, PRKCD, DYRK1A, DYRK1B, CSNK1D, PGD, CDC25A, AR, CCNE2, CCNE1, PLAA, ABCG2, DNMT1, KLK1, TXK, PIK3R1, HIF1A, ACACB, NUA1, TERT, LYN, VDR, PLK1, CDC7, BRAF, ESR1, ESR2, PTK2, CLK1, CDK4, CDK2, BCL2, MDM2, CDK1, MDM4, FGFR1, TOP2A, ACHE, GSK3B, FLT4, PIK3CB, POLB, JAK2, JAK1, HSP90AA1, DUSP3, PARP1, SYK, MMP2, TYK2, SREBF2, CCNA2, NCOR2, CCNA1, PPARG, TOP1, SGK1, PPARA, PPARD, HDAC4, HDAC5, HDAC2, HDAC3, PCNA, SRC, NR1I3, PTGS2, TYMS, EGFR, AURKB, HDAC7, PTGS1, AURKA, RXRA, ERBB2, MAPK1, MAPK3, NOS2, STAT1, NR1H2, AKR1C3, NR1H3, PTPN11, MAPK14, MTOR, WEE1, FABP4, RPS6KB1, APEX1, PTPN6, PTPN2</i>
GO:0005737~cytoplasm	107	0.005336642	<i>APP, HDAC10, PREP, NR3C1, RPS6KA3, PNP, CCND1, RPS6KA1, PIM1, AKT1, MAP3K8, PIM3, PIM2, PDGFRB, G6PD, PRKCH, PRKCB, PRKCE, PRKCD, CDC25A, CDC25B, ERN1, AR, ADAM17, PLAA, PTGFR, TXK, PIK3R1, PLA2G7, HIF1A, NUA1, LYN, PLK1, CDC7, BRAF, ESR1, PTK2, CDK9, CLK1, CDK2, BCL2, MDM2, CDK1, MAP3K14, BCL2L1, TOP2A, GSK3B, FLT4, HTR2B, AKR1B1, PIK3CG, POLB, CA1, CA3, CA2, JAK2, ACP1, JAK1, HSP90AA1, DUSP3, NPY5R, SYK, TYK2, ADRA2C, SREBF2, ADRA2A, CCNA2, MMP14, MAPT, SGK1, FBP1, PLEC, HDAC4, HDAC5, HDAC2, HDAC3, PCNA, SRC, NR1I3, ODC1, PTGS2, TYMS, EGFR, HDAC7, PTGS1, HSD17B1, ERBB2, MAPK1, AOC3, GABBR1, NOS2, STAT1, NR1H2, AKR1C3, PTPN11, MAPK14, MTOR, VEGFA, FABP1, WEE1, FABP4, RPS6KB1, FABP5, APEX1, PTPN6, TEK, HSPA1A</i>
GO:0016021~integral component of membrane	101	0.026736903	<i>APP, CISD1, COMT, ATP12A, IGF1R, ADORA3, ADORA1, KDR, CYP1B1, CA14, PTGDR, PDGFRB, KCNH2, TAAR1, GABRG2, AR, MTNR1A, ADAM17, MTNR1B, AGTR1, PTGES, ABCG2, PTGFR, SLC22A6, ABCB1, MAOB, MAOA, CHRNA7, SLC5A2, CYP19A1, FUT4, HSD11B1, HSD11B2, EBP, FUT7, NPC1L1, ST3GAL3, FDFT1, CCR1, TAS2R31, SRD5A1, ESR1, SQUE, PTPRC, TBXAS1, CYP1A2, BCL2, NOX4, ALPL, DHCR7, BCL2L1, FGFR1, ALK, GABRB2, ACHE, HTR2B, ECE1, SLC6A2, PTPRF, SLC6A4, GRM2, CA4, CA9, ACP1, ABCC1, PTGIR, GPR35, SIGMAR1, AVPR1A, TACR1, ADRA2C, BACE1, FCER2, BACE2, MMP14, MMP13, KCNMA1, MET, UGT2B7, PTGER4, HDAC2, PTGER1, PTGER2, PTGER3, HMGR, EGFR, GLRA1, CXCR1, CNR1, ERBB2, HSD17B2, CA12, AOC3, BCHE, PTPN1, GABRA1, GABBR1, CYP51A1, OPRK1, SCD, PTPN2</i>

Table V: Top 20 hub genes with the highest degree score

No	Gene symbol	Full name	Score
1	<i>AKT1</i>	Serine/threonine-protein kinase AKT	123
2	<i>MAPK3</i>	MAP kinase ERK1	116
3	<i>EGFR</i>	Epidermal growth factor receptor erbB1	107
4	<i>SRC</i>	Tyrosine-protein kinase SRC	102
5	<i>MAPK1</i>	MAP kinase ERK3	101
6	<i>VEGFA</i>	Vascular endothelial growth factor A	98
7	<i>HSP90AA1</i>	Heat shock protein HSP 90-alpha	90
8	<i>ESR1</i>	Estrogen receptor alpha	84
9	<i>PTGS2</i>	Cyclooxygenase-2	82
10	<i>MTOR</i>	Serine/threonine-protein kinase mTOR	76
11	<i>PIK3CA</i>	PI3-kinase p110-alpha subunit	74
12	<i>APP</i>	Beta-amyloid A4 protein	65
13	<i>MMP9</i>	Matrix metalloproteinase 9	62
14	<i>MAPK14</i>	MAP kinase p38 alpha	59
15	<i>AR</i>	Androgen Receptor	58
16	<i>ERBB2</i>	Receptor protein-tyrosine kinase erbB-2	57
17	<i>MDM2</i>	p53-binding protein Mdm-2	57
18	<i>KDR</i>	Vascular endothelial growth factor receptor 2	56
19	<i>BCL2L1</i>	Apoptosis regulator Bcl-X	55
20	<i>STAT1</i>	Signal transducer and activator of transcription 1-alpha/beta	55

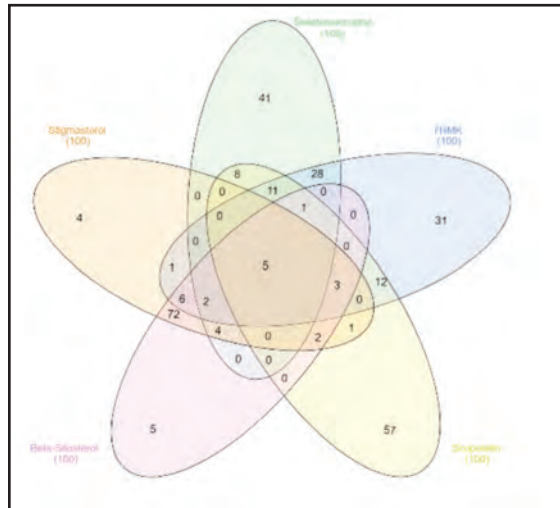


Fig. 1: Venn diagram of predicted genes target of 5 potential mahogany compounds, resulting in 294 potential targets.

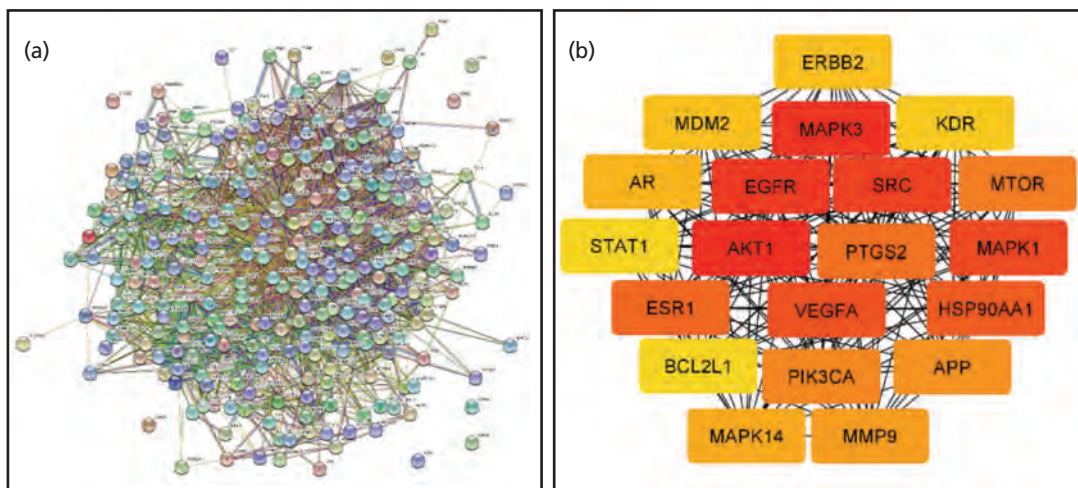


Fig. 2: (a) Protein-protein interaction networks of predictive mahogany metabolite target genes analyzed using STRING-DB and (b) the top 20 hub genes with the highest degree score analyzed using Cytoscape.

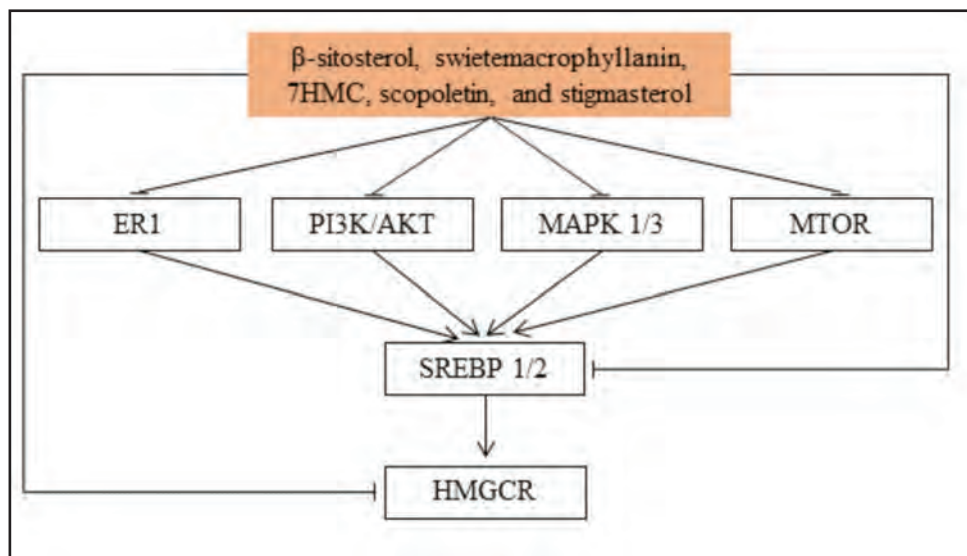


Fig. 3: Mechanism of antidiabetic activity of the 5 mahogany test compounds through the direct inhibition of HMGCR and indirect inhibition through SREBP, ER1, PI3K/AKT, MAPK 1/3, and MTOR.

target of mahogany compounds (Table II). SREBP was activated by MAPK, AKT1, PI3K, MTOR, and ER1.²⁸⁻³⁰

Intracellular mitogen-activated protein kinases (MAPKs) are an essential class of proline-dependent protein kinases involved in regulating various biological functions, such as inflammation, cell proliferation, and differentiation.³¹ MAPK1 and MAPK3 (also known as ERK2 and ERK1, respectively) are the members of the MAPK family. The N-terminal domains of SREBP1a, SREBP1c, and SREBP2 are the substrates of MAPK1 and MAPK3.³² The activation of the MAP kinase cascade increases the transcriptional activity of SREBP1a and SREBP2 to a similar degree (state). MAPK1/3 plays a role in regulating the lipid metabolism in the liver.³³ A past study also confirmed that the inhibition of MAPK3 had been known to reduce adipocytes and resistance to high-fat diet-induced obesity due to impaired adipocyte differentiation and higher postprandial metabolism.³⁴

The phosphatidylinositol 3-kinase/protein kinase B (PI3K/AKT) pathway is considered as one of the upstream pathways of SREBP.²⁹ The Akt pathway positively modulates the activation of SREBP2, which selectively activates *de novo* cholesterol synthesis.³⁵ The inhibition of the AKT signaling pathway is known to inhibit the formation of SREBP2 and the downstream target genes of SREBP2, such as LDLR and HMGCR.³⁵

The mechanistic target of rapamycin (mTOR) is the catalytic subunit of two structurally distinct complexes: mTORC1 and mTORC2, both of which localize to different subcellular compartments and also affect different activation and function.³⁶ During obesity and overnutrition conditions, mTORC1 is hyperactivated, resulting in the persistent activation of SREBP 1c in the liver, leading to the overproduction of lipids and hepatic steatosis hypertriglyceridemia.³⁷ The inhibition of mTORC1 is known to reduce the SREBP2 activity and cholesterol synthesis in the endoplasmic reticulum.²⁸ Moreover, the inhibition of mTORC1 is known to prevent lipid storage processes, increase low-density lipoprotein cholesterol levels, and activate lipolysis.³⁸ Thus, the inhibition of mTORC1 can be a potential therapeutic target for metabolic syndromes such as dyslipidemia.

Estrogen receptor alpha (ER α) plays a significant role in adipocyte activity and sexual dimorphism in fat distribution.⁷ For instance, ER α modulates the process of transcription and the activation of proteins that play a role in fat metabolisms, such as PPAR gamma, SREBP, HMGCR, and LDLR.^{25,30,39} Past research has shown that ER-alpha activation plays a role in activating the SREBP2 expression, which is correlated with the exhibition of the HMGCR expression for cholesterol synthesis and LDLR for the cellular uptake of LDL cholesterol.^{30,40} However, past studies have shown that phytoestrogen genistein activation of SREBP2 did not significantly increase HMGCR expression, rather it increases LDLR expression.⁴⁰

Our research suggests that mahogany contains β -sitosterol, swietemachropyllanin, swietenia, 7-HMC, and scopoletin, which are responsible for the estrogenic and anti-dyslipidemic activity with the mechanism through direct or indirect inhibition of HMGCR. Indirect inhibition of the

HMGCR activity through inhibition of the ERK1/2, AKT/PI3K, mTOR, and estrogen receptor alpha pathways mediated through SREBP1/2 (Fig. 3). This study demonstrates the potential of mahogany as an estrogenic agent and a dyslipidemia-preventing agent in postmenopausal women. This research was based on bioinformatics research that suspected the compound roles of its activity and mechanism pathways. Therefore, further research is warranted to confirm our results.

CONCLUSION

In this study, a network pharmacology approach was proposed to explore the mechanism underlying the action of mahogany on dyslipidemia for menopausal conditions. The active ingredients of mahogany in the treatment of dyslipidemia consisted of five compounds β -sitosterol, swietemachropyllanin, 7-hydroxy-2-(4-hydroxy-3-methoxyphenyl)-chroman-4-one (7HMC), scopoletin, and stigmasterol. The possible molecular mechanisms mainly involved the direct inhibitory pathway of HMGCR and the indirect inhibitory pathway of HMGCR. The indirect inhibitory pathway was mediated through the PI3K/AKT, MAPK1/3, MTOR, ER1, and SREBP1/2 signaling pathways. Our findings suggested the use of mahogany as an alternative herbal therapy to prevent dyslipidemia in menopause conditions and exert estrogenic activity. This research provides new insights for further research on the anti-dyslipidemic effect of mahogany.

ACKNOWLEDGMENTS

Thanks to *Program Kreativitas Mahasiswa 2020 (PKM 2020)* from the Directorate of Learning and Student Affairs, Ministry of Education and Culture of the Republic of Indonesia, for funding this research. We are also grateful to Prof. Dr. apt. Edy Meiyanto, M.Si, for excellent discussion and suggestion while finishing this study.

REFERENCES

1. Santoro N, Worsley R, Miller KK, Parish SJ, Davis SR. Role of estrogens and estrogen-like compounds in female sexual function and dysfunction. *J Sex Med* 2016; 13(3): 305–16.
2. Yeasmin N, Akhter QS, Mahmuda S, Nahar S, Rabbani R, Hasan M, et al. Effect of estrogen on serum total cholesterol and triglyceride levels in postmenopausal women. *Journal of Dhaka Medical College* 2017; 26(1): 25–31.
3. Dalal PK, Agarwal M. Postmenopausal syndrome. *Indian J Psychiatry* 2015; 57(2): S222–32.
4. Fait I. Menopause hormone therapy: latest developments and clinical practice [cited Sep 2020]. Available from: <https://www.ncbi.nlm.nih.gov/pmc/articles/PMC6317580/>.
5. Davidson MH, Maki KC, Karp SK, Ingram KA. Management of hypercholesterolaemia in postmenopausal women. *Drugs Aging*. 2002; 19(3): 169–78.
6. Kuiper GG, Lemmen JG, Carlsson B, Corton JC, Safe SH, van der Saag PT, et al. Interaction of estrogenic chemicals and phytoestrogens with estrogen receptor beta. *Endocrinology* 1998; 139(10): 4252–63.
7. Lizcano F, Guzmán G. Estrogen deficiency and the origin of obesity during menopause. *Biomed Res Int* 2014; 757461.
8. Ness GC, Chambers CM. Feedback and hormonal regulation of hepatic 3-hydroxy-3-methylglutaryl coenzyme A reductase: the concept of cholesterol buffering capacity. *Proc Soc Exp Biol Med* 2000; 224(1): 8–19.

9. Ko S-H, Kim H-S. Menopause-associated lipid metabolic disorders and foods beneficial for postmenopausal women. *Nutrients* 2020; 12(1): 202.
10. Moghadamtousi SZ, Goh BH, Chan CK, Shabab T, Kadir HA. Biological activities and phytochemicals of *Swietenia macrophylla* King. *Molecules* 2013; 18(9): 10465–83.
11. Goh BH, Kadir HA. In vitro cytotoxic potential of *Swietenia macrophylla* King seeds against human carcinoma cell lines. *JMPR* 201; 5(8): 1395–404.
12. Hasibuan PAZ, Sitanggang RG, Angkat RS. Estrogenic Activity of mahoni seed ethanolic extract [*Swietenia mahogany* (L.) Jacq] on uterus weight, bone density and mammae gland proliferation on ovariectomized rats. *Indonesian Journal of Cancer Chemoprevention* 2020; 11(2): 75–83.
13. Lau WK, Goh BH, Kadir HA, Shu-Chien AC, Tengku Muhammad TS. Potent PPAR γ ligands from *swietenia macrophylla* are capable of stimulating glucose uptake in muscle cells. *Molecules* 2015; 20(12): 22301–14.
14. Ayunda RD, Prasetyastuti P, Hastuti P. Effect of 7-hydroxy-2-(4-hydroxy -3-methoxyphenyl)-chroman-4-one on level of mangan-superoxide dismutase (mn-sod) and superoxide dismutase 2 (sod2) gene expression in hyperlipidemia rats. *Indonesian Journal of Pharmacy* 2019; 30(3):180.
15. Kalpana K, Pugalendi KV. Antioxidative and hypolipidemic efficacy of alcoholic seed extract of *Swietenia macrophylla* in streptozotocin diabetic rats [cited Aug 2020]. Available from: <https://www.degruyter.com/view/j/jbcpp.2011.22.issue-1-2/jbcpp.2011.001/jbcpp.2011.001.xml>
16. Cerqueira NMFSA, Oliveira EF, Gesto DS, Santos-Martins D, Moreira C, Moorthy HN, et al. Cholesterol biosynthesis: A mechanistic overview. *Biochemistry* 2016; 55(39): 5483–506.
17. DeBose-Boyd RA. Feedback regulation of cholesterol synthesis: Sterol-accelerated ubiquitination and degradation of HMG CoA reductase. *Cell Res* 2008; 18(6): 609–21.
18. Sydow D, Morger A, Driller M, Volkamer A. TeachOpenCADD: A teaching platform for computer-aided drug design using open source packages and data [cited Mar 2021]. Available from: <https://www.ncbi.nlm.nih.gov/pmc/articles/PMC6454689/>
19. Wulandari F, Ikawati M, Meiyanto E, Kirihata M, Hermawan A. Bioinformatic analysis of CCA-1.1, a novel curcumin analog, uncovers furthest noticeable target genes in colon cancer. *Gene Reports* 2020; 21: 100917.
20. Hermawan A, Putri H, Utomo RY. Functional network analysis reveals potential repurposing of β -blocker atenolol for pancreatic cancer therapy. *DARU J Pharm Sci* 2020; 28(2): 685–99.
21. Chin C-H, Chen S-H, Wu H-H, Ho C-W, Ko M-T, Lin C-Y. cytoHubba: identifying hub objects and sub-networks from complex interactome. *BMC Syst Biol* 201; 8: S11.
22. Nicola G, Berthold MR, Hedrick MP, Gilson MK. Connecting proteins with drug-like compounds: Open source drug discovery workflows with BindingDB and KNIME [cited May 2021]. Available from: <https://doi.org/10.1093/database/bav087>
23. Ben-David A. About the relationship between ROC curves and Cohen's kappa. *Engineering Applications of Artificial Intelligence* 2008; 21(6): 874–82.
24. Yelaware Puttaswamy N, Urooj A. In vivo antihypercholesterolemic potential of *swietenia mahagoni* leaf extract. *Cholesterol* 2016; 2016: e2048341.
25. Trapani L, Pallottini V. Age-related hypercholesterolemia and HMG-CoA reductase dysregulation: Sex Does Matter (A Gender Perspective) [cited Sep 2020]. Available from: <https://www.ncbi.nlm.nih.gov/pmc/articles/PMC2863156/>
26. Wu N, Sarna LK, Hwang S-Y, Zhu Q, Wang P, Siow YL, et al. Activation of 3-hydroxy-3-methylglutaryl coenzyme A (HMG-CoA) reductase during high fat diet feeding. *Biochimica et Biophysica Acta (BBA) - Molecular Basis of Disease* 2013; 1832(10): 1560–8.
27. DeBose-Boyd RA, Ye J. SREBPs in lipid metabolism, insulin signaling, and beyond. *Trends Biochem Sci* 2018; 43(5): 358–68.
28. Eid W, Dauner K, Courtney KC, Gagnon A, Parks RJ, Sorisky A, et al. mTORC1 activates SREBP-2 by suppressing cholesterol trafficking to lysosomes in mammalian cells. *PNAS* 2017; 114(30): 7999–8004.
29. Krycer JR, Sharpe LJ, Luu W, Brown AJ. The Akt-SREBP nexus: cell signaling meets lipid metabolism. *Trends in Endocrinology & Metabolism* 2010; 21(5): 268–76.
30. Meng Y, Zong L. Estrogen stimulates SREBP2 expression in hepatic cell lines via an estrogen response element in the SREBP2 promoter. *Cellular & Molecular Biology Letters* 2019 Dec; 24(1): 65.
31. Upadhya D, Ogata M, Reneker LW. MAPK1 is required for establishing the pattern of cell proliferation and for cell survival during lens development. *Development* 2013 Apr; 140(7): 1573–82.
32. Roth G, Kotzka J, Kremer L, Lehr S, Lohaus C, Meyer HE, et al. MAP kinases Erk1/2 phosphorylate sterol regulatory element-binding protein (SREBP)-1a at serine 117 in vitro. *Journal of Biological Chemistry* 2000; 275(43): 33302–7.
33. Xiao Y, Liu H, Yu J, Zhao Z, Xiao F, Xia T, et al. Activation of ERK1/2 ameliorates liver steatosis in leptin receptor-deficient (db/db) mice via stimulating ATG7-dependent autophagy. *Diabetes* 2016; 65(2): 393–405.
34. Bost F, Aouadi M, Caron L, Even P, Belmonte N, Prot M, et al. The Extracellular signal-regulated kinase isoform ERK1 Is specifically required for in vitro and in vivo adipogenesis. *Diabetes* 2005; 54(2): 402–11.
35. Luu W, Sharpe LJ, Stevenson J, Brown AJ. Akt acutely activates the cholesterolgenic transcription factor SREBP-2. *Biochimica et Biophysica Acta (BBA) - Molecular Cell Research* 2012; 1823(2): 458–64.
36. Wullschlegel S, Loewith R, Hall MN. TOR Signaling in Growth and Metabolism. *Cell* 2006; 124(3): 471–84.
37. Ai D, Baez JM, Jiang H, Conlon DM, Hernandez-Ono A, Frank-Kamenetsky M, et al. Activation of ER stress and mTORC1 suppresses hepatic sortilin-1 levels in obese mice. *J Clin Invest* 2012; 122(5): 1677–87.
38. Xie X, Zhang L, Li X, Liu W, Wang P, Lin Y, et al. Liangxue Jiedu Formula Improves Psoriasis and Dyslipidemia Comorbidity via PI3K/Akt/mTOR Pathway. *Front Pharmacol* 2021; 12: 591608.
39. Jeong S, Yoon M. 17 β -Estradiol inhibition of PPAR γ -induced adipogenesis and adipocyte-specific gene expression. *Acta Pharmacologica Sinica* 2011; 32(2): 230–8.
40. Kartawijaya M, Han HW, Kim Y, Lee S-M. Genistein upregulates LDLR levels via JNK-mediated activation of SREBP-2. *Food Nutr Res* 2016; 60: 10.3402/fnr.v60.31120.
21. Patel M, Chan CC. Immunopathological aspects of age-related macular degeneration. *Seminars in Immunopathology* 2008; 30: 97–110.
22. WuZ, Lauer TW, Sick A, Hackett SF, Campochiaro PA. Oxidative stress modulates complement factor H expression in retinal pigmented epithelial cells by acetylation of FOXO3. *J Biol Chem* 2007; 282: 22414–25.
23. Beatty S, Koh H, Phil M, Henson D, Boulton M. The role of oxidative stress in the pathogenesis of age-related macular degeneration. *Surv Ophthalmol* 2000; 45: 115–34.
24. Nishibori T, Tanabe Y, Su L, David M. Impaired development of CD4⁺ CD25⁺ regulatory T cells in the absence of STAT1: increased susceptibility to autoimmune disease. *J Exp Med* 2004; 199: 25–34.
25. Iannaccone A, Neeli I, Krishnamurthy P, Lenchik NI, Wan H, Gerling IC, et al. Autoimmune biomarkers in age-related macular degeneration: A possible role player in disease development and progression. *Adv Exp Med Biol* 2012; 723: 11–6.
26. Morohoshi K, Goodwin AM, Ohbayashi M, Ono SJ. Autoimmunity in retinal degeneration: Autoimmune retinopathy and age-related macular degeneration. *J Autoimmun* 2009; 33: 247–54.